Predicting Polarization and Nonlinear Dielectric Response of Arbitrary Perovskite Superlattice Sequences

Xifan Wu,[1] Massimiliano Stengel,[2] Karin M. Rabe,[3] and David Vanderbilt[3]
[1]*Chemistry Department, Princeton University, Princeton, New Jersey 08544-0001, USA*
[2]*Materials Department, University of California, Santa Barbara, California 93106-5050, USA*
[3]*Department of Physics and Astronomy, Rutgers University, Piscataway, New Jersey 08854-8019, USA*
(Received 22 May 2008; published 18 August 2008)

We carry out first-principles calculations of the nonlinear dielectric response of short-period ferroelectric superlattices. We compute and store not only the total polarization, but also the Wannier-based polarizations of individual atomic layers, as a function of the electric displacement field, and use this information to construct a model capable of predicting the nonlinear dielectric response of an arbitrary superlattice sequence. We demonstrate the successful application of our approach to superlattices composed of $SrTiO_3$, $CaTiO_3$, and $BaTiO_3$ layers.

DOI: 10.1103/PhysRevLett.101.087601 PACS numbers: 77.22.Ej, 77.80.−e, 77.84.Lf

The development of advanced methods for layer-by-layer epitaxial growth of multicomponent perovskite superlattice structures has generated excitement [1], both because of the intriguing materials physics that comes into play and because of potential applications in nonvolatile ferroelectric memories, piezoactuators and sensors, and magnetoelectric devices [2]. To guide experimental exploration of this greatly expanded class of materials, there is a critical need for atomic-scale understanding and modeling of key structural and functional properties, particularly polarization and dielectric response.

First-principles methods have allowed for the direct quantitative computation of such material-specific information for representative perovskite superlattices [3,4]. However, such calculations are limited to relatively short-period superlattices, of the order of 10 unit cells. First-principles *modeling* can extend our theoretical capability so that one can make predictions about arbitrary stacking sequences and elucidate the physics behind the novel behavior of superlattices. In particular, substantial progress has recently been made in isolating and studying the effects of the epitaxial strain on film structure, polarization, and piezoelectric properties [5,6].

It is clear, however, that it is electrostatic effects that dominate the physics of superlattices built from ferroelectric (e.g., $BaTiO_3$) and incipient ferroelectric (e.g., $SrTiO_3$) constituents. In previous first-principles models, these effects were included in an approximate way, either by describing the layers in terms of their bulk linear dielectric properties [3], or by imposing a constant-polarization layer-to-layer constraint that only roughly captures the effects of the internal electric fields [7]. Furthermore, most previous first-principles calculations, using the periodic boundary conditions implicit in ordinary implementations, give results only for zero applied electric field. Since much of the interest in perovskite superlattices lies in their use in capacitor structures whose performance relies on their nonlinear dielectric behavior under bias voltage, a more fundamental methodology capable of capturing such effects is urgently needed.

In this Letter, we present a rigorous first-principles treatment allowing computation and modeling of the nonzero electric-field response of perovskite oxide superlattices. Our approach is based on a recently developed Wannier-based formulation of the layer polarizations in perovskite superlattices [8] in combination with methods for treating insulators in finite electric fields [9–12]. Crucially, we choose to work at fixed electric *displacement* field [13], and show that this gives a clean separation between long-range Coulomb interactions and short-range interfacial effects. As we demonstrate through application to superlattices composed of three ABO_3 perovskite constituents, the resulting model yields, for arbitrary stacking sequences, quantitative predictions of polarization and nonlinear dielectric response with *ab initio* accuracy, thus enabling the theory-driven search of the full range of superlattice sequences for novel or optimized properties.

The construction of our model begins with the decomposition of the superlattice into atomic layers, specifically into AO and BO_2 layers alternating along [001]. The individual layer polarizations (LP) for each AO and BO_2 layer j are computed using the Wannier-based method of Ref. [8], and recorded as functions $p_j(D)$ of the displacement field D using a constrained-D first-principles implementation [13]. This choice is appropriate because (i) D is constant throughout the supercell ($\nabla \cdot \mathbf{D} = 4\pi\rho_{\text{free}} = 0$), while the local macroscopic $\mathcal{E}$ and P generally vary, and (ii) imposing constant-D electrical boundary conditions has the virtue of making the force-constant matrix of the quasi-one-dimensional superlattice short-ranged in real-space. This ''locality principle'' implies that one may expect the $p_j(D)$ to depend only on the *local* compositional environment comprising the layer itself and few nearby neighbors. For any given superlattice, the total polariza-

tion, which is a quantity of central interest, is given by $P(D) = c(D)^{-1}\sum_j p_j(D)$ where $c(D)$ is the relaxed superlattice periodicity. It is also straightforward to obtain the electric equation of state in other forms, e.g., $D(P)$ by numerical inversion, and $\mathcal{E}(P) = D(P) - 4\pi P$.

We demonstrate the method through application to superlattices composed of an arbitrary sequence of $SrTiO_3$, $BaTiO_3$, and $CaTiO_3$ layers, grown in the (001) direction with an in-plane lattice constant $a_0 = 7.275$ bohr, our theoretical equilibrium lattice constant of bulk $SrTiO_3$. We assume 1×1 in-plane periodicity and tetragonal $P4mm$ symmetry, thus neglecting possible intermixing, nanodomain formation, or the appearance of antiferroelectric or octahedral-tilting distortions. Consistent with the $P4mm$ symmetry, D is taken along the z axis, ranging in steps from -0.32 to 0.32 C/m^2.

First-principles calculations to optimize the structure for fixed D [13] and to obtain the layer polarizations $p_j(D)$ and lattice constants $c(D)$ were performed on a database of superlattices using the LAUTREC code package, which implements plane-wave calculations in the projector augmented-wave framework [14] in the local-density approximation [15]. The polarization and its coupling to the electric field is handled by an efficient real-space Wannier formulation [12]. We used a plane-wave energy cutoff of 40 Ry and a $6 \times 6 \times 2$ Monkhorst-Pack k mesh. The database of superlattice structures contains all one- and two-component period-4 supercells (*BBBB*, *SSSS*, *CCCC*, *BBBS*, *BBSS*, *BSBS*, *BSSS*, *CCCS*, *CCSS*, *CSCS*, *CSSS*, *BBBC*, *BBCC*, *BCBC*, *BCCC*), and one three-component superlattice *SSBC*, where *C*, *S*, and *B* refer to $CaTiO_3$, $SrTiO_3$, and $BaTiO_3$ layers, respectively.

Representative $p_j(D)$ curves are presented in Fig. 1. It is striking that the LP curves separate, as expected from our locality principle, into clusters depending on the nearest-layer chemical environment (color-coded for comparison). However, the differences among the curves within a cluster are still too large to neglect, especially for TiO_2 layers, indicating that an accurate model must include further-neighbor interactions as well. The effects of local inversion symmetry breaking are also clearly visible. For example, a BaO layer in the middle of a *CBB* sequence has a large and positive LP even at $D = 0$. Smaller shifts arise from the second-neighbor environment, e.g., for the central TiO_2 layer in a *BBSS* sequence.

We now introduce a cluster expansion [16] for the environment dependence of the $p_l(\{s\}; D)$ as

$$p_l(\{s\}) = J_0 + \sum_i (J_{l,i} s_i + J'_{l,i} s_i^2) + \sum_{ij} (J_{l,ij} s_i s_j + J'_{l,ij} s_i s_j^2 + J''_{l,ij} s_i^2 s_j^2) + \sum_{ijk} J_{l,ijk} s_i s_j s_k + \cdots, \quad (1)$$

where the J are D-dependent effective cluster interactions (ECI) to be determined from fitting to the first-principles database. We choose "spin" variables $s_i = -1, 0$, and 1 to identify *AO* layer i as CaO, SrO, and BaO, respectively, to reflect the fact that Sr is midway between Ca and Ba in the periodic table. Thus, insofar as Sr acts like an average of Ca and Ba atoms, each appearance of a squared spin variable s^2 in a term of the cluster expansion makes it more likely that the term can be neglected.

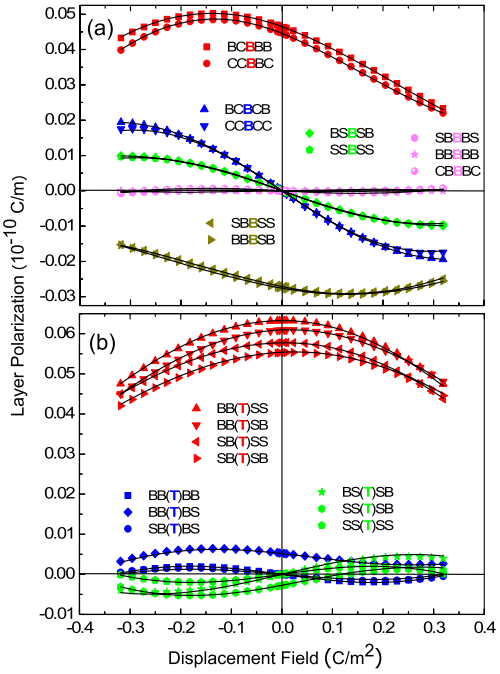

FIG. 1 (color online). Dependence of layer polarizations on chemical environment for (a) BaO planes (relative to a BaO plane in bulk $BaTiO_3$) and (b) TiO_2 planes (relative to an average of TiO_2 planes in bulk $BaTiO_3$ and $SrTiO_3$). *C*, *S*, *B*, and *T* refer to CaO, SrO, BaO, and TiO_2 layers, respectively. First-principles results and model fittings are denoted by symbols and solid lines, respectively.

We therefore approached the truncation and fitting of the model of Eq. (1) with three principles in mind: (i) the importance of an n-body term is expected to decrease rapidly with n; (ii) the dependence of p_l on s_i should decay rapidly with the distance between layers l and i; and (iii) coefficients with prime superscripts, corresponding to "higher-level" spin variables s^2, should be less important than those without.

Translation and spatial-inversion symmetry imply that $J_{l,l+m}(D) = -J_{l,l-m}(-D)$, $J_{l,l+m,l+n}(D) = -J_{l,l-m,l-n}(-D)$, etc., independent of l. It is therefore natural to define $\mathcal{J}_m = (J_{l,l-m} + J_{l,l+m})/2$ and $\tilde{\mathcal{J}}_m = (J_{l,l-m} - J_{l,l+m})/2$, and similarly for two-body and higher terms. Correspondingly, we separate Eq. (1) into parts $p^{(-)}_{AO}(D)$ and $p^{(-)}_{TiO_2}(D)$ that are odd in D, and parts $p^{(+)}_{AO}(D)$ and $p^{(+)}_{TiO_2}(D)$ that are even in D, reflecting the inversion-symmetry-conserving and inversion-symmetry-breaking characters of the local environment, respectively. To give a sense of the form of the resulting expressions, the odd part for *AO* layers becomes

TABLE I. Fitted linear-in-D term of effective cluster interactions for AO layers as defined in Eq. (2).

	ECI	Value	ECI	Value
Zero body	$\mathcal{J}$	2.2771		
One body	$\mathcal{J}_0$	0.1113	$\mathcal{J}'_0$	0.0819
	$\mathcal{J}_1$	0.0034	$\mathcal{J}'_1$	0.0007
	$\mathcal{J}_2$	−0.0018		
Two body	$\mathcal{J}_{01}$	0.0197	$\mathcal{J}_{02}$	0.0031
	$\mathcal{J}_{\bar{1}1}$	0.0026	$\mathcal{J}_{12}$	0.0013

$$p_{AO}^{(-)} = \mathcal{J} + \mathcal{J}_0 s_0 + \mathcal{J}'_0 s_0^2 + \mathcal{J}_1(s_{\bar{1}} + s_1) + \mathcal{J}'_1(s_{\bar{1}}^2 + s_1^2) + \mathcal{J}_2(s_{\bar{2}} + s_2) + \mathcal{J}_{01}(s_{\bar{1}} s_0 + s_0 s_1) + \mathcal{J}_{02}(s_{\bar{2}} s_0 + s_0 s_2) + \mathcal{J}_{\bar{1}1} s_{\bar{1}} s_1 + \mathcal{J}_{12}(s_{\bar{2}} s_{\bar{1}} + s_1 s_2), \quad (2)$$

where $\bar{n} = -n$ and layer 0 is the one whose LP is being expanded. Similar expressions for $p_{AO}^{(+)}$, $p_{\mathrm{TiO}_2}^{(-)}$, and $p_{\mathrm{TiO}_2}^{(+)}$ are given in the supplementary material [17]. The supercell lattice constant $c(D)$ is correspondingly expanded as

$$c = \sum_j (\mathcal{C}_1 + \mathcal{C}_2 s_j + \mathcal{C}_3 s_j^2 + \mathcal{C}_4 s_j s_{j+1}), \quad (3)$$

where $\mathcal{C}_1(D)$, $\mathcal{C}_2(D)$, and $\mathcal{C}_3(D)$ assign to each layer its bulk $c(D)$, and only the $\mathcal{C}_4(D)$ term includes true superlattice effects. The $\mathcal{J}(D)$ and $\mathcal{C}(D)$ parameters are expressed as fifth- and fourth-order Taylor expansions in D, respectively, with the Taylor coefficients obtained by fitting to the first-principles calculations of $p_j(D)$ and $c(D)$ for superlattices in the database.

The choice of terms to include in Eq. (2) and in the corresponding expressions for $p_{AO}^{(+)}$, $p_{\mathrm{TiO}_2}^{(-)}$, and $p_{\mathrm{TiO}_2}^{(+)}$ [17] have been obtained using linear regression techniques. The linear-in-D coefficients of the ECIs in Eq. (2) are presented in Table I, confirming our expectation that terms of higher body, longer range, and higher level tend to be less important. Tables listing values of all of the ECI coefficients are provided in the supplementary material [17].

The quality of the fit is excellent; the overall rms error in $p_j(D)$ values relative to first-principles results is 2×10^{-14} C/m for structures in the database. This is illustrated in Fig. 1, where the solid lines representing the fitted functions can be seen to pass quite accurately through the first-principles symbols. The quality of the fit is similar for other cases, not plotted.

The model can now be used to predict the nonlinear dielectric and piezoelectric properties of arbitrary superlattice sequences. To illustrate the quality of the fit for supercell configurations that were *not* included in the fit, we compare in Fig. 2 the first-principles $P(\mathcal{E})$ curves with the model fits for the tricolor $1S1B2C$ supercell. The $P(\mathcal{E})$ curves are seen to be in excellent agreement. The arrows in Fig. 2 indicate $\mathcal{E} = 0$ solutions corresponding to $P = -P_s$ in the preferred (stable) phase, $P = P_{\mathrm{unst}}$ at the unstable saddle point, and $P = P_{\mathrm{meta}}$ in the metastable phase. Note that $|P_s| \neq |P_{\mathrm{meta}}|$ and $P_{\mathrm{unst}} \neq 0$ because the superlattice has broken inversion symmetry. The model predicts P_s, P_{unst}, and P_{meta} values of −0.19, 0.04, and 0.16 C/m^2, to be compared with direct first-principles values of −0.20, 0.04, and 0.16 C/m^2, respectively. While the inversion-symmetry-breaking effects are subtle, they are critical for tuning certain ferroelectric properties [18,19], and it is gratifying that they are obtained accurately by our model.

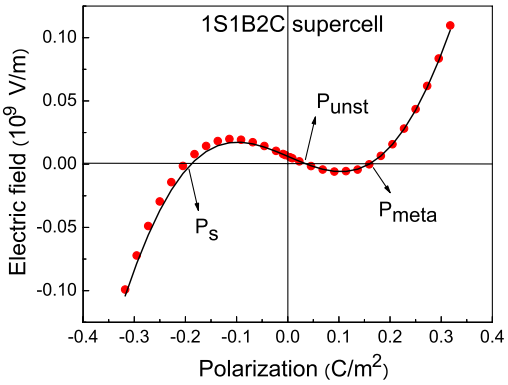

FIG. 2 (color online). Model prediction (solid lines) and first-principles calculations (symbols) of $\mathcal{E}$ vs P for $1S1B2C$ superlattice.

To demonstrate the ability of our model to predict properties of long-period superlattices that would be impractical for direct first-principles calculations, we present our model predictions for $nSnBnC$ superlattices in Table II. Because of the broken inversion symmetry, one polarization direction is favored, with a different magnitude, over the other. The polarizations approach the bulk value of 0.274 C/m^2 for large n, but with decreasing n we find a progressive suppression of the polarization and an enhancement of the asymmetry until, at $n = 1$, the system becomes paraelectric, with a single minimum. These effects are also evident in the static dielectric response curves (including the piezoelectrically mediated component) shown in Fig. 3, obtained by plotting $(d\mathcal{E}/dD)^{-1}$ vs $\mathcal{E}(D)$ parametrically as functions of D. It is clear that the curves lack reflection symmetry about the vertical axis, and the system is seen to cross from ferroelectric to paraelectric behavior between $n = 2$ and $n = 1$.

To gain more insight into interface effects in these superlattices, we can characterize each of the six kinds of interfaces by an interface dipole, extracted from our first-principles model as follows. Using S/B as an example, we

TABLE II. Predicted magnitude of polarization (C/m^2) for preferred (P_s) and metastable (P_{meta}) polarization states in $nSnBnC$ superlattices.

	$n = 1$	$n = 2$	$n = 4$	$n = 8$	$n = \infty$
P_s	−0.040	−0.198	−0.250	−0.267	−0.274
P_{meta}		0.178	0.237	0.262	0.274

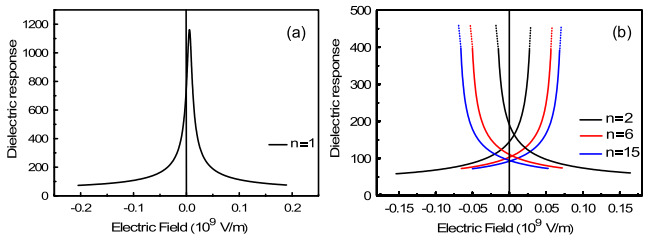

FIG. 3 (color online). Dielectric response of *nSnBnC* superlattice in (a) paraelectric and (b) ferroelectric regime.

imagine an infinite stack $\ldots SSSBBB\ldots$ with one interface, and define $p_{\mathrm{int}}(D) = \sum_i p_i(D) - p_i^{(0)}(D)$, where i runs over AO and TiO_2 layers, $p_i(D)$ is the actual layer polarization predicted by our model, and $p_i^{(0)}(D)$ is the polarization of that layer type in its own bulk environment. [For the central TiO_2 layer, $p^{(0)}(D)$ is the average of the bulk S and B values.] Because of the short-range nature of the model, the sum only needs to run over a few layers near the interface.

The resulting $p_{\mathrm{int}}(D)$ curves are presented in Fig. 4. First, note that the curves tend to have a negative slope at $D = 0$ and thus contribute an interface dipole of opposite sign to D for small D; this reflects the fact that the presence of interfaces tends to suppress the ferroelectricity, as was also evident in Table II and Fig. 3. Second, each pair such as BS and SB are related by the symmetry $p_{\mathrm{int}}^{BS}(D) = -p_{\mathrm{int}}^{SB}(-D)$ required by the condition that the overall $P(D)$ of a bicolor *nSnB* superlattice must be odd in D. Third, the inversion symmetry breaking, relevant to tricolor superlattices such as *nBnSnC*, is evident in the failure of the $p_{\mathrm{int}}^{BS}(D) + p_{\mathrm{int}}^{SC}(D) + p_{\mathrm{int}}^{CB}(D)$ curve to pass through the origin in the inset of Fig. 4.

The utility of the interface dipole concept is that, for any superlattice in which the interfaces are never separated by less than three unit cells (as determined by the range of our model), $P(D)$ can be calculated just by summing the bulk contribution for each layer and then adding the contribution from each interface. This prescription yields a simplified but equivalent model that can be used in such cases.

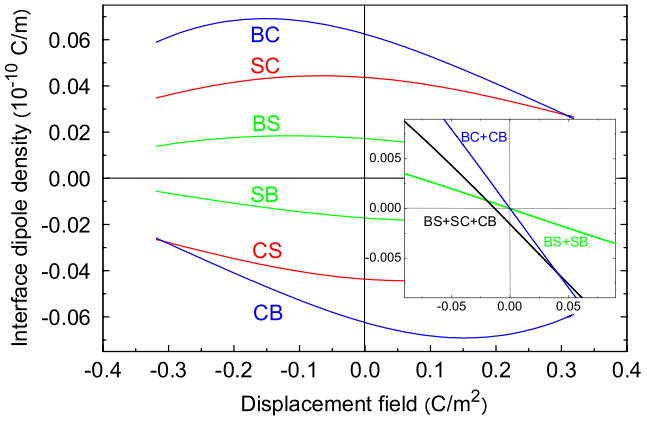

FIG. 4 (color online). Model interface dipole densities.

Thus, for example, the inversion-symmetry-breaking effects in *lBmSnC* superlattices are captured exactly by the simplified prescription as long as $l, m, n \geq 3$.

In summary, we have shown how a model can be extracted from first-principles calculations on short-period superlattices and used to make quantitatively accurate predictions of nonlinear dielectric and piezoelectric responses over a range of applied fields for arbitrary superlattice sequences. The treatment of electrostatic effects is rigorous, a key aspect being the choice of the displacement field as the fundamental electrical variable so as to keep interlayer interactions short-ranged. The approach can be straightforwardly generalized to include dependence on epitaxial strain. Such an approach can play an important role in enabling the design of multifunctional ferroelectric superlattices with desired polarization, piezoelectric, or dielectric responses.

This work was supported by ONR Grants No. N00014-05-1-0054 and No. N0014-00-1-0261, and ARO-MURI Grant No. W91NF-07-1-0410.

[1] M. Dawber, K. M. Rabe, and J. F. Scott, Rev. Mod. Phys. **77**, 1083 (2005).
[2] J. F. Scott, Science **315**, 954 (2007).
[3] J. B. Neaton and K. M. Rabe, Appl. Phys. Lett. **82**, 1586 (2003).
[4] E. Bousquet *et al.*, Nature (London) **452**, 732 (2008).
[5] O. Diéguez, K. M. Rabe, and D. Vanderbilt, Phys. Rev. B **72**, 144101 (2005).
[6] D. Schlom, L. Chen, C. Eom, K. M. Rabe, S. K. Streiffer, and J. Triscone, Annu. Rev. Mater. Res. **37**, 589 (2007).
[7] S. M. Nakhmanson, K. M. Rabe, and D. Vanderbilt, Phys. Rev. B **73**, 060101(R) (2006).
[8] X. Wu, O. Diéguez, K. M. Rabe, and D. Vanderbilt, Phys. Rev. Lett. **97**, 107602 (2006).
[9] I. Souza, J. Íñiguez, and D. Vanderbilt, Phys. Rev. Lett. **89**, 117602 (2002).
[10] P. Umari and A. Pasquarello, Phys. Rev. Lett. **89**, 157602 (2002).
[11] O. Diéguez and D. Vanderbilt, Phys. Rev. Lett. **96**, 056401 (2006).
[12] M. Stengel and N. A. Spaldin, Phys. Rev. B **75**, 205121 (2007).
[13] M. Stengel, N. A. Spaldin, and D. Vanderbilt (to be published).
[14] P. E. Blöchl, Phys. Rev. B **50**, 17953 (1994).
[15] J. P. Perdew and Y. Wang, Phys. Rev. B **45**, 13244 (1992).
[16] A. Zunger, *Statics and Dynamics of Alloy Phase Transformations*, edited by P. E. A. Turchi and A. Gonis (Plenum, New York, 1994), pp. 361–419.
[17] See EPAPS Document No. E-PRLTAO-101-040833 for details of the fitted effective cluster interactions that fully specify the model. For more information on EPAPS, see http://www.aip.org/pubservs/epaps.html.
[18] H. N. Lee, H. M. Christen, M. F. Chisholm, C. M. Rouleau, and D. H. Lowndes, Nature (London) **433**, 395 (2005).
[19] N. Sai, B. Meyer, and D. Vanderbilt, Phys. Rev. Lett. **84**, 5636 (2000).